Research Square

Preprints are preliminary reports that have not undergone peer review.
They should not be considered conclusive, used to inform clinical practice,
or referenced by the media as validated information.

BIS-Based Model Reference Adaptive Control of Anesthesia Depth under Patient Variability and Time-Varying Delays

Raha Rahimi
Isfahan University of Technology
Marzieh Kamali
Isfahan University of Technology
Fazaneh Shayegh
Isfahan University of Technology
Zahra Baharlouei
zahra.bahar@res.mui.ac.ir

Isfahan University of Medical Sciences

Article

Keywords: Closed-loop anesthesia, Model reference adaptive control, Bispectral index, Time-varying delay, Propofol-remifentanil infusion, Pharmacokinetic/pharmacodynamic modeling

Posted Date: August 3rd, 2026

DOI: https://doi.org/10.21203/rs.3.rs-9871286/v1

License: This work is licensed under a Creative Commons Attribution 4.0 International License.
Read Full License

Additional Declarations: No competing interests reported.

Version of Record: A version of this preprint was published at Scientific Reports on November 13th, 2026. See the published version at https://doi.org/10.1038/s41598-026-78511-4.

BIS-Based Model Reference Adaptive Control of Anesthesia Depth under Patient Variability and Time-Varying Delays

Raha Rahimi [1], Marzieh Kamali [1], Fazaneh Shayegh [1], Zahra Baharlouei [2*]

[1] *Department of Electrical and Computer Engineering, Isfahan University of Technology, Isfahan 84156-83111, Iran.*

[2] *Medical Image and Signal Processing Research Center, School of Advanced Technologies in Medicine, Isfahan University of Medical Sciences, Isfahan, Iran.*

* *Corresponding author: Zahra Baharlouei, E-mail address:* zahra.bahar@res.mui.ac.ir

Abstract

General anesthesia plays a critical role in modern surgical care, requiring accurate regulation of hypnotic and analgesic drug administration to maintain unconsciousness and analgesia. A major challenge in anesthesia control is the presence of significant inter-patient variability and physiological time-varying delays. Conventional control approaches often rely on manual tuning or patient-specific parameter identification, limiting their applicability in real clinical settings. This study proposes a Model Reference Adaptive Control (MRAC) strategy for automated closed-loop regulation of anesthesia depth using propofol and remifentanil. The proposed framework incorporates a Pharmacokinetic/Pharmacodynamic model and compensates for nonlinear drug-response behavior through an inverse Hill-function approach. A key advantage of the proposed adaptive controller is its independence from patient-specific tuning and prior parameter identification, enabling real-time personalized anesthesia management without model recalibration. Simulation results on a heterogeneous virtual patient population demonstrate settling times of approximately 4–6 min during induction with minimal overshoot (<5%). The Bispectral Index (BIS) was successfully maintained within the clinically acceptable range of 40–60, with an average value close to 50 and small deviations (±2). Compared with previously reported anesthesia control strategies, the proposed MRAC approach achieves competitive tracking performance while maintaining stable tracking across heterogeneous patients and time-varying delays. These findings suggest that the proposed strategy provides a promising solution for robust and individualized closed-loop anesthesia management.

Keywords: Closed-loop anesthesia, Model reference adaptive control, Bispectral index, Time-varying delay, Propofol-remifentanil infusion, Pharmacokinetic/pharmacodynamic modeling

1. Introduction

The process of administering general anesthesia encompasses complex pharmacological interactions aimed at ensuring unconsciousness, analgesia, and physiological stability during surgical procedures. The key components of anesthesia are hypnosis, which suppresses consciousness, and analgesia, which blocks pain perception [1,2]. General anesthesia fundamentally depends on the essential components of hypnosis and analgesia, which must be precisely induced, maintained, and balanced to secure patient unconsciousness and adequate analgesia. Therefore, the simultaneous and balanced administration of these components is fundamental for safe and effective general anesthesia [3].

Propofol, with rapid onset, is widely used to induce and maintain hypnosis. Remifentanil, an ultra-fast-acting opioid, is commonly combined with propofol for balanced anesthesia. Their precise titration remains challenging: underdosing risks awareness and pain, while overdosing may cause cardiovascular or respiratory complications [4–7]. General anesthesia proceeds through induction, maintenance, and emergence;

drugs are initiated to induce unconsciousness, titrated under continuous monitoring to maintain intraoperative stability, and discontinued to permit recovery while minimizing complications [8,9].

Automated drug delivery systems improve precision, reduce workload, and enhance patient outcomes [10,11]. The Bispectral Index (BIS), derived from EEG, provides continuous and objective monitoring of anesthesia depth (0–100 scale), with 40–60 indicating adequate general anesthesia. Real-time BIS feedback enables precise adjustment of agents such as propofol, reducing risks of awareness or oversedation and supporting safe recovery [12]. Traditionally, anesthetic dosing relied on clinicians' manual adjustments based on vital signs. Studies indicate that automated anesthesia systems outperform manual methods by delivering more consistent anesthetic depth, reducing overall drug consumption, and improving safety [13–15]. However, BIS monitoring signals may be corrupted by measurement noise, artifacts, and signal quality degradation in clinical environments, which can reduce the reliability of feedback-based anesthesia systems [16]. Therefore, the automated anesthesia system should be sufficiently robust to maintain stable performance under such disturbances and measurement uncertainties.

To further enhance precision in anesthesia delivery, mathematical modeling techniques have been increasingly integrated into clinical practice. These models integrate patient-specific characteristics including age, body weight, height, and gender, allowing for more individualized drug delivery and improving the precision of predicted responses. In particular, Pharmacokinetic/Pharmacodynamic (PK/PD) models describe the relation between drug dynamics and effects, providing the basis for personalized anesthesia protocols [17,18]. These models enable individualized administration of propofol and remifentanil, supporting advanced control strategies [19].

However, a common assumption in PK/PD modeling is that drug distribution between compartments occurs instantaneously. While this may be acceptable in simplified scenarios, it often fails to capture the physiological delays present in real systems particularly in the context of anesthetic drug administration. In fact, in many conventional PK/PD formulations, time delays in drug distribution are not explicitly incorporated, which may affect real-world closed-loop performance. In practice, following drug injection, a finite amount of time is required for the drug to reach different compartments, such as extracellular and intracellular spaces. Neglecting these temporal dynamics reduces model fidelity and limits its ability to accurately describe the system's transient behavior. Physiological changes such as reduced cardiac output further alter drug distribution, increasing the risk of instability. Therefore, to enable safe and effective control of anesthesia, it is essential to incorporate system delays and memory effects into PK-PD models [20–22].

Early target-controlled infusion (TCI) systems relied on PK models to administer drugs at predefined target concentrations [23]. But as open-loop systems, they could not adapt to individual patient responses. Feedback-based control strategies have significantly improved the automation and precision of anesthesia management. Unlike conventional systems that deliver anesthetic drugs at a fixed, predetermined rate, closed-loop systems dynamically adjust drug administration based on continuous monitoring of the patient's depth of anesthesia. The benefits of employing closed-loop control in anesthesia are substantial. These systems enhance patient safety, reduce drug consumption, shorten recovery time, and minimize adverse effects, thereby improving the overall quality of medical care. Moreover, due to their ability to adapt to the patients physiological changes, closed-loop systems are particularly well-suited for patients with complex and variable clinical conditions [24,25].

A variety of closed-loop control approaches have been developed to regulate the Depth of Hypnosis (DoH) in general anesthesia. As an illustration, a feedforward BIS-guided anesthesia control strategy was presented in [26], combining an optimized induction bolus with PID-based propofol infusion regulation. An

event-driven PID control scheme was proposed in [11] to jointly regulate propofol and remifentanil infusion, with real-time BIS feedback guiding dose adjustments. While effective, these PID methods still rely on fixed PK/PD model parameters and therefore lack adaptability to inter-patient variability. A physiologically-based Model Predictive Control (MPC) framework was presented in [27] for automated regulation of anesthesia and analgesia through the coadministration of propofol and remifentanil using BIS and MAP measurements. Another nonlinear Multi Input Single Output (MISO) MPC strategy was introduced in [28] to predict drug interactions and optimize BIS tracking under safety constraints. Although MPC-based approaches have demonstrated promising performance in anesthesia regulation, their effectiveness depends on the availability of patient models and online prediction accuracy, which may limit robustness under significant inter-patient variability and physiological uncertainty. A Higher Order Sliding Mode Controller (HOSMC) was presented in [29] for automated propofol infusion. Although robust against parameter variations and surgical disturbances, this approach remains dependent on an assumed PK/PD model parameters, which limits its performance under unmodeled dynamics. More recently, a Fractional-Order Model Reference Adaptive Control (FOMRAC) framework was proposed in [30], leveraging fractional calculus to account for long-memory effects in anesthesia dynamics. Despite its stability guarantees, the controller does not explicitly incorporate physiological delays, which are clinically significant during altered cardiac output or slow drug exchange.

This study formulates an MRAC framework tailored to anesthesia systems subject to time-varying delays, with the objective of addressing the previously mentioned challenges. The key contributions of this work are outlined below:

- Our MRAC approach for delayed anesthesia systems does not require exact patient-specific PK/PD parameter identification for controller implementation, eliminating the need for prior parameter identification or patient-specific tuning required in conventional and event-based PID controllers [11].
- Unlike existing adaptive frameworks such as FOMRAC [30], the proposed method explicitly incorporates physiological time-varying delays in the PK dynamics, allowing more accurate control under conditions such as reduced cardiac output or delayed drug transport.
- The proposed adaptive controller regulates the dose infusion dynamics of propofol and remifentanil within clinically accepted standard ranges, thereby enhancing patient safety during surgery and supporting a smooth postoperative recovery by preventing both overdosing and insufficient drug administration.
- To compensate for the nonlinear Hill function of the PK/PD model and resolve the ambiguity associated with the combined drug effect, a simplified inverse Hill reconstruction is proposed by approximating the normalized remifentanil effect as proportional to the normalized propofol effect. This formulation enables reconstruction of the estimated linear output from the BIS signal and facilitates adaptive output-feedback control despite the nonlinear multi-drug interaction.
- The adaptive law continuously updates the control parameters online, enhancing robustness against inter-patient variability and intraoperative disturbances, while avoiding controller retuning or recalibration during surgery.

The paper proceeds as follows. Section 2 details the patient models for propofol and remifentanil, incorporating the effects of system delays. Section 3 details the proposed adaptive control strategy. Simulation results are presented and analyzed in Section 4. Conclusions and key observations are provided in Section 5.

2. PK/PD patient model

The PK/PD framework used in this study provides a realistic yet simplified representation of the pharmacological effects of propofol and remifentanil during anesthesia [31]. Both drugs are represented by standard three-compartment PK models (Schnider [32]), describing plasma and tissue distribution. The PK part predicts blood drug concentration over time and simulates processes such as absorption, distribution, and elimination, which are generally modeled linearly. The pharmacodynamic component links the effect-site concentration to the BIS output and is commonly modeled with a nonlinear Hill function [19,33].

Drug interaction is included to capture the synergistic effect whereby remifentanil reduces propofol requirements [34]. This is modeled with a Hill function including a coefficient β, which quantifies the strength of the synergistic interaction between propofol and remifentanil [35]. Figure 1 illustrates the standard PK/PD block diagram used in this work.

It is worth noting that the pharmacokinetic structures of propofol and remifentanil are identical, as both drugs are modeled using a standard three-compartment representation. The main difference arises in the pharmacodynamic component, particularly in the effect-site dynamics and drug-specific sensitivity parameters. In the controller design, the formulation is developed based on the propofol model without loss of generality. Due to the structural similarity between the two drug models, the same control framework can be directly extended to determine the remifentanil infusion rate.

The pharmacokinetic behavior of both propofol and remifentanil is described using standard three-compartment linear models, as introduced in Schnider [36,37]. The corresponding model equations with time-varying delay for propofol is expressed as

$$\begin{cases} \dot{x}_1(t) = -(k_{10} + k_{12} + k_{13})x_1(t) + k_{21}x_2(t - \tau(t)) + k_{31}x_3(t - \tau(t)) + \dfrac{1}{V_1}u_p(t), \\ \dot{x}_2(t) = k_{12}x_1(t) - k_{21}x_2(t), \\ \dot{x}_3(t) = k_{13}x_1(t) - k_{31}x_3(t), \end{cases} \tag{1}$$

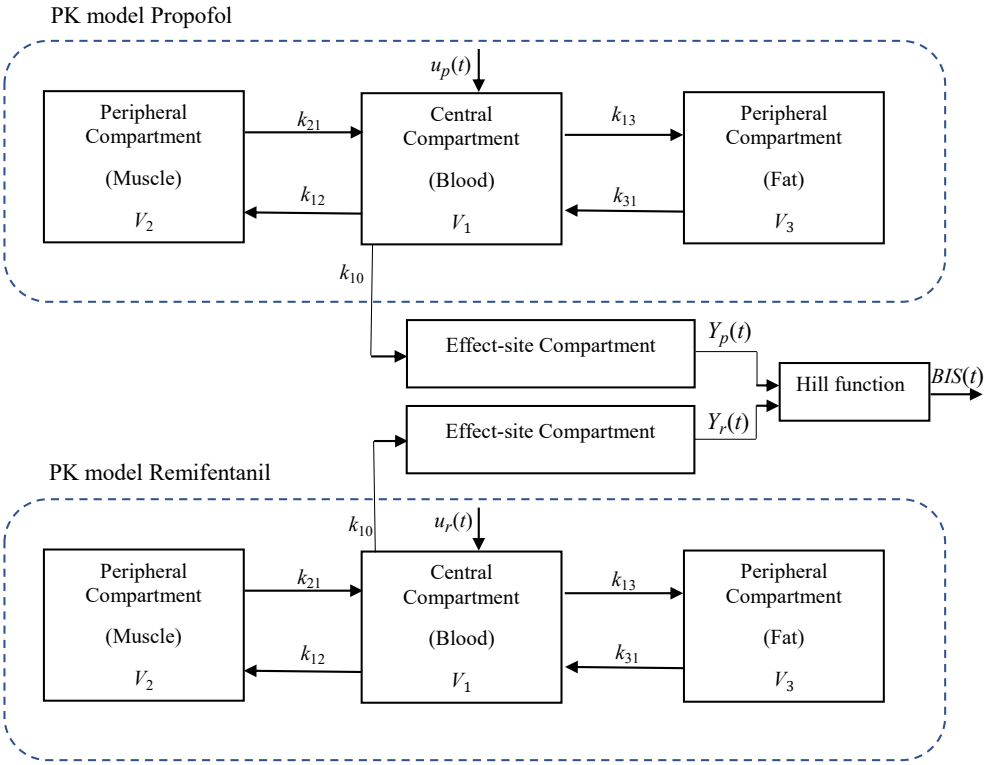


Fig. 1. Block diagram of the PK-PD model.

where x_1, x_2 and x_3 denote central and peripheral drug concentrations respectively, with k_{ij} $[1/min]$ the inter-compartmental transfer rates, V_1 the central volume, and $u_p(t)$ the infusion rate of propofol. The pharmacokinetic model for remifentanil follows the same structure as given in (1), with the input term replaced by $u_r(t)$, representing the infusion rate of remifentanil. The parameters k_{ij} $[1/min]$ for the pharmacokinetic component of propofol can be determined using Table I. In this Table, V_i $[l]$, CL_i $[\frac{l}{min}]$, and LBM $[kg]$ represents the volume of the ith compartment, the elimination clearance associated with the i-th compartment, along with lean body mass respectively.

Remark 1 It should be noted that since we use adaptive controller, the exact numerical values of these parameters are not required for controller implementation. Unlike most existing approaches, they are only used in simulation to reproduce inter-patient variability, while the same control structure can be uniformly applied across different subjects.

The time-varying delay $\tau(t)$ is assumed to be bounded and continuously differentiable, satisfying

$$0 < \tau(t) < \tau_{max}, \quad \dot{\tau}(t) \leq \bar{\tau} < 1, \tag{2}$$

where τ_{max} is assumed to be known. In the PK/PD framework of general anesthesia, the delay varies within the range of 50 to 70 seconds, which satisfies the above condition. This assumption ensures that the proposed adaptive control and stability analysis remain valid under the considered physiological delay variations.

Table I. The parameters of the PK component [31].

Parameter	Calculation
LBM for males	$1.1(weight\ [kg]) - 128\left(\frac{weight\ [kg]^2}{height\ [cm]^2}\right)$
LBM for females	$1.07(weight\ [kg]) - 148\left(\frac{weight\ [kg]^2}{height\ [cm]^2}\right)$
k_{10} , k_{12} , k_{13}	$\frac{Cl1}{V_1}$, $\frac{Cl2}{V_1}$, $\frac{Cl3}{V_1}$
k_{21} , k_{31}	$\frac{Cl2}{V_2}$, $\frac{Cl3}{V_3}$
CL_1	$1.89 + 0.0456(weight[kg] - 77)$ - $0.0681\ (LBM\ [kg]\ -59)$ + $0.0264\ (height\ [cm] - 177)$
CL_2	$1.29 - 0.024\ (age\ [year] - 53)$
CL_3	0.836
V_1	4.27
V_2	$18.9 - 0.391\ (age\ [year] - 53)$
V_3	2.38

The effect-site concentration for propofol and remifentanil denoted by $X_{e,p}(t)$ $[mg/ml]$ and $X_{e,r}(t)$ $[mg/ml]$, respectively, are modeled as virtual compartments linked to the plasma concentration. Their dynamics are described by

$$\dot{X}_{e,p}(t) = 0.459\ ((\frac{x_1(t)}{V_1}) - X_{e,p}(t)), \tag{3}$$

$$\dot{X}_{e,r}(t) = (0.595 - 0.007(Age - 40))(\frac{x_1(t)}{V_1} - X_{e,r}(t)). \tag{4}$$

The BIS response is described by a Hill function

$$BIS(t) = E_0 - E_{max}\left(\frac{\left(\frac{Y_p(t) + Y_r(t)}{U_{50}(\phi)}\right)^{\gamma}}{1 + \left(\frac{Y_p(t) + Y_r(t)}{U_{50}(\phi)}\right)^{\gamma}}\right), \tag{5}$$

where E_0, E_{max}, and γ denote the baseline BIS level, the maximum drug effect, and the sensitivity parameter, respectively. Following [28], $Y_p(t)$ and $Y_r(t)$ represent the normalized effect-site concentrations of propofol and remifentanil, obtained from $X_{e,p}(t)$ and $X_{e,r}(t)$ with respect to their corresponding 50% effective concentrations $X_{e_{50},p}$ and $X_{e_{50},\mathrm{r}}$, which define the drug levels required to achieve half of the maximum pharmacological effect resulting in

$$Y_p(t) = \frac{X_{e,p}(t)}{X_{e_{50},p}}, \quad Y_r(t) = \frac{X_{e,r}(t)}{X_{e_{50},\mathrm{r}}}. \tag{6}$$

The drug interaction term $U_{50}(\phi)$, is defined by

$$U_{50}(\phi) = 1 - \beta\phi + \beta\phi^2, \tag{7}$$

where the co-administration ratio ϕ and synergy coefficient β, accounts for the enhanced hypnotic effect of combined drugs and

$$\phi(t) = \frac{Y_p(t)}{Y_p(t) + Y_r(t)}, \tag{8}$$

represents the combined pharmacological effect of the two drugs. The resulting BIS output is between 0 (absence of detectable cortical activity) and 100 (awake).

The PK/PD model with time-varying delays developed in this section provides the foundation for designing an adaptive controller. For this purpose, the subsequent sections will address three main tasks: (i) compensating for the nonlinear drug interaction through inversion of the Hill function, (ii) develop a delay-compensating MRAC law that does not rely on patient-specific parameters or explicit delay values and is capable of handling patient variability, and (iii) performing a stability analysis using a Lyapunov-Krasovskii framework. These steps directly tackle the key challenges of nonlinear dynamics, physiological delays, and considerable patient-to-patient variability in closed-loop anesthesia systems.

3. Proposed Control Method

This section introduces an MRAC-based control framework for uncertain nonlinear systems with time-delay effects, tailored to the PK/PD anesthesia model. The overall control architecture is depicted in Fig. 2, where the proposed MRAC scheme regulates the infusion of propofol and remifentanil. The corresponding patient dynamics are represented by P_p and P_r, while the nonlinear drug interaction is captured by the Hill function H. According to [28], a fixed ratio M between propofol and remifentanil is introduced to resolve the inherent ambiguity of the multi-input anesthesia system. Since the BIS index alone cannot uniquely determine the contribution of each drug, imposing this clinically motivated constraint ensures a well-defined control problem and prevents unrealistic drug allocation. In the proposed closed-loop configuration, the patient block includes two parallel PK/PD channels corresponding to propofol and remifentanil. The outputs of these channels are denoted by Y_p(t) for propofol and $Y_r(t)$ for remifentanil, representing their respective effect-site responses. These outputs are processed through the nonlinear Hill function H to generate the BIS estimate produced by the plant. The resulting BIS signal corresponds to the modeled hypnotic response of the patient.

To reflect intraoperative conditions, an external disturbance $d(t)$, representing surgical stimuli or nociceptive events, is added to the BIS output during the maintenance phase [13,30]. Consequently, the measurable BIS signal provided to the controller is expressed as

$$BIS_m(t) = BIS(t) + d(t), \tag{9}$$

In this MRAC approach, the controller's parameter vector is continuously updated through an adaptive law, allowing the controller to adjust its parameters in real time to meet the desired performance objectives. The reference input $r(t)$ is set to maintain a target BIS value of 50, with $W_m(s)$ representing the reference model that produces desired output $y_m(t)$. The reference model defines the desired closed-loop dynamics of the anesthesia system. In contrast to a simple step input that specifies only the steady-state target, the reference model characterizes the full transient behavior, including rise time, overshoot, and settling time, which the adaptive controller aims to track. This formulation ensures clinically acceptable performance during both transient and steady-state conditions, while remaining independent of patient-specific variability.

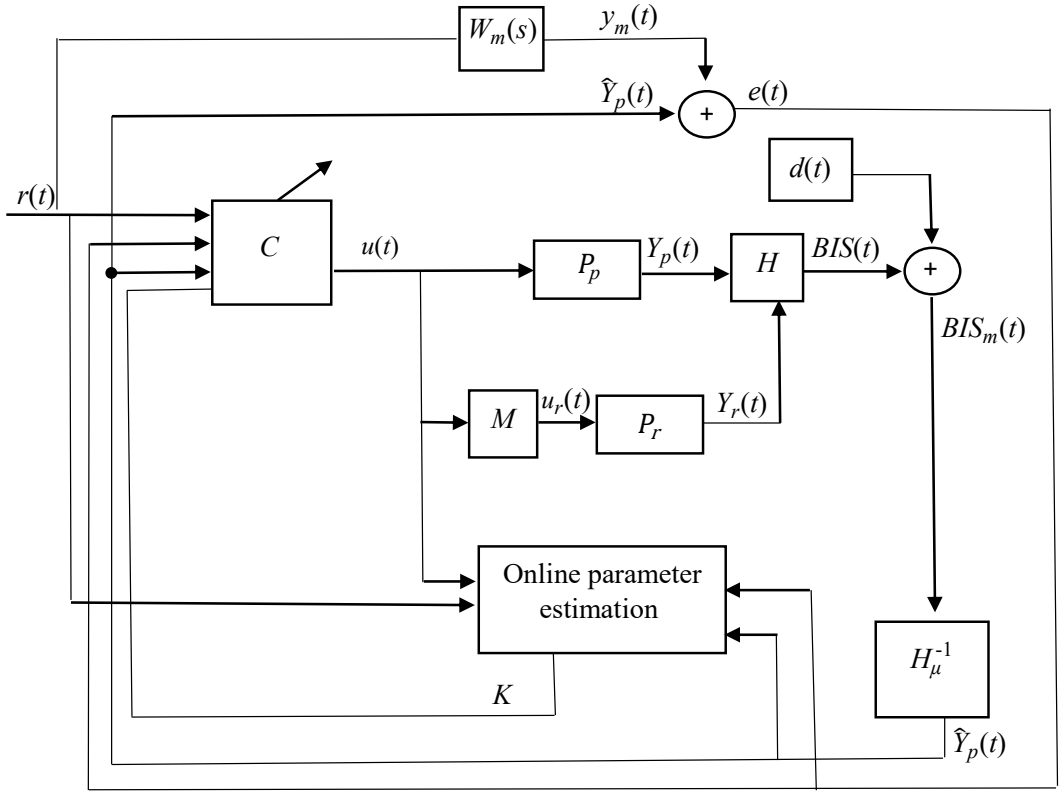


Fig. 2. Closed loop anesthesia control system.

Due to the nonlinear nature of the Hill function, the tracking error is defined based on the output of the linear propofol dynamics, denoted by $Y_p(t)$. Since $Y_p(t)$ is not directly measurable, it is estimated using inverse Hill function H_μ^{-1} and its estimate $\hat{Y}_p(t)$ is used in the controller. Therefore, the tracking error, defined as $e(t) \triangleq \hat{Y}_p(t) - y_m(t)$, measures the difference between the estimated plant output and the reference model output. This error serves as a critical metric for assessing how accurately the system follows the desired trajectory. Minimizing this error using MRAC controller ensures that the system output aligns closely with the target response.

3.1 Inversion of the Hill function

Since the controller requires a linear feedback variable while the BIS output is generated through a nonlinear multi-drug Hill relationship, a novel inverse reconstruction strategy is introduced to simplify the nonlinear multi-drug interaction dynamics. Specifically, the inverse function H_μ^{-1} is employed to compensate for the Hill nonlinearity and reconstruct the estimated normalized propofol effect-site concentration, $\hat{Y}_p(t)$, which is then used as the feedback variable in the control process.

For control-oriented simplification, the normalized remifentanil effect-site concentration is assumed to be approximately proportional to the normalized propofol effect-site concentration, i.e.,

$$Y_r(t) \approx \mu Y_p(t), \tag{10}$$

where $\mu > 0$ represents the relative contribution of remifentanil to the overall anesthetic effect. This approximation is introduced for control design purposes and is not intended to represent an exact physiological equality between the two drug effects. Therefore,

$$Y_p(t) + Y_r(t) = (1 + \mu)Y_p(t), \tag{11}$$

and the interaction ratio becomes

$$\phi(t) = \frac{Y_p(t)}{Y_p(t) + Y_r(t)} = \frac{1}{1+\mu}. \tag{12}$$

Consequently, the drug interaction term $U_{50}(\phi)$ becomes constant and can be written as

$$U_{50}(\mu) = 1 - \frac{\beta}{1+\mu} + \frac{\beta}{(1+\mu)^2}. \tag{13}$$

Substituting these relations into the Hill function yields a single-variable nonlinear relation between the BIS signal and $Y_p(t)$,

$$BIS(t) = E_0 - E_{max}\left(\frac{\left(\frac{(1+\mu)Y_p(t)}{U_{50}(\mu)}\right)^{\gamma}}{1+\left(\frac{(1+\mu)Y_p(t)}{U_{50}(\mu)}\right)^{\gamma}}\right). \tag{14}$$

Since $Y_p(t)$ is not directly measurable, its estimate is reconstructed from the measured BIS signal as

$$\hat{Y}_p(t) = \frac{U_{50}(\mu)}{1+\mu}\left(\frac{E_0 - BIS_m(t)}{E_{max} - E_0 + BIS_m(t)}\right)^{1/\gamma}. \tag{15}$$

This reconstructed variable is then used as the feedback signal for the adaptive controller.

3.2 Controller design

In general, the overall system dynamics, including both PK and PD components for propofol, can be represented as

$$\dot{x}_1(t) = -(k_{10} + k_{12} + k_{13})x_1(t) + k_{21}x_2(t - \tau(t)) + k_{31}x_3(t - \tau(t)) + \frac{1}{V_1}u_p(t), \tag{16}$$

$$\dot{x}_2(t) = k_{12}x_1(t) - k_{21}x_2(t),$$

$$\dot{x}_3(t) = k_{13}x_1(t) - k_{31}x_3(t),$$

$$\dot{X}_{e,p}(t) = 0.459\left(\left(\frac{x_1(t)}{V_1}\right) - X_{e,p}(t)\right).$$

The controller design procedure is developed for propofol. However, the same methodology can be directly applied to remifentanil, as both drugs follow an identical modeling and control framework. For notational simplicity, in the following development, the propofol infusion rate $u_p(t)$ is denoted as $u(t)$. The plant dynamics of propofol are represented by a linear state-space model given by

$$\dot{x}(t) = Ax(t) + Ba_\tau^{*T}x(t - \tau(t)) + Bu(t), \tag{17}$$

$$Y_p(t) = cx(t),$$

$$A = \begin{bmatrix} -(k_{10}+k_{12}+k_{13}) & 0 & 0 & 0 \\ 0 & -k_{21} & 0 & 0 \\ 0 & 0 & -k_{31} & 0 \\ \frac{0.459}{V_1} & 0 & 0 & -0.459 \end{bmatrix},$$

$$a_\tau^{*T} = [0 \quad V_1 k_{21} \quad V_1 k_{31} \quad 0],$$

$$B = \left[\frac{1}{V_1} \quad 0 \quad 0 \quad 0\right]^T,$$

$$c = \left[0 \quad 0 \quad 0 \quad \frac{1}{X_{e_{50},p}}\right].$$

where $x(t) \in \Re^4$ denotes the system state vector, $Y_p(t) \in \Re$ represents the plant output, and $u(t) \in \Re$ is the control input and $\tau(t)$ is the unknown time-varying delay in the PK/PD model.
Typically, first the transfer function of the system without delay is considered, upon which the solution for the delayed case is subsequently developed. The transfer function of (16) without delay is

$$Y_p(t) = G_p(s)u(t), \quad G_p(s) = \frac{1}{V_1}\frac{(s+k_{21})(s+k_{31})}{(s+m_1)(s+m_2)(s+m_3)} \times \frac{0.459}{s+0.459} = \frac{k_p N(s)}{D(s)}, \tag{18}$$

where

$$k_p = \frac{0.459}{V_1}, \tag{19}$$

$$N(s) = (s+k_{21})(s+k_{31}),$$

$$D(s) = (s+m_1)(s+m_2)(s+m_3)(s+0.459),$$

denote the numerator, and denominator polynomials of the transfer function $G_p(s)$ of system without delay, respectively, and k_p is the high-frequency gain. The coefficients m_1, m_2, m_3 are related to the underlying PK rate constants [10],

$$m_1 + m_2 + m_3 = k_{10} + k_{12} + k_{13} + k_{21} + k_{31}, \tag{20}$$

$$m_1 m_2 + m_1 m_3 + m_2 m_3 = k_{10}(k_{21}k_{31}) + k_{31}(k_{12}k_{21}) + k_{13}k_{21},$$

$$m_1 m_2 m_3 = k_{10} k_{21} k_{31}.$$

The transfer function of the reference model is

$$y_m(t) = W_m(s)r(t), \quad W_m(s) = \frac{1}{D_m(s)}, \tag{21}$$

where $D_m(s)$ is a monic Hurwitz polynomial of degree two.
The conditions required for the design of the adaptive controller are examined in the following:

1. All pharmacokinetic and pharmacodynamic parameters are positive ($V_1, k_{ij} > 0$), therefore, the plant transfer function without delay is minimum-phase and the sign of the high-frequency gain k_p is known.

2. Based on (18), the transfer function of system without delay has a relative degree of two, defined as the difference between the number of poles and zeros. For consistency in controller design, the plant and the reference model are selected to have identical relative degrees [38]; therefore, the relative degree of $W_m(s)$ is also chosen to be two.

Inspired by the MRAC design approaches proposed in [38–40] for systems with relative degree two, the adaptive control law is derived here. Accordingly, we first construct the model reference controller for the system without considering delay, assuming that the parameters in (1) are known. Using this control law, the error equation is then derived. Subsequently, based on the error equation, the controller is designed for the system with unknown parameters and time-varying delay.

Now $u^*(t)$ is designed in standard form for the system without delay and with unknown parameters according to

$$u(t) = u^*(t) = K_1^{*T}\omega_1(t) + K_2^{*T}\omega_2(t) + K_e^*\hat{Y}_p(t) + K_r^* r(t), \tag{22}$$

$$\omega_1(t) = F(s)u(t) \in \Re^3, \quad \omega_2(t) = F(s)\hat{Y}_p(t) \in \Re^3, \tag{23}$$

$$F(s) = \frac{\alpha(s)}{\Lambda(s)}, \quad \alpha(s) \triangleq \alpha_2(s) = [s^2 \quad s \quad 1]^T, \tag{24}$$

where K_1^*, $K_2^* \in \Re^3$, $K_e^* \in \Re$, $K_r^* \in \Re$ are controller parameters and $\Lambda(s)$ is a monic third-order Hurwitz polynomial. To handle the relative-degree-two plant within a standard MRAC framework, a stable filter is introduced. The role of $F(s)$ is to generate strictly proper filtered regressors, which allows us to construct an adaptive controller based on filtered versions of the input and output signals rather than on their unfiltered forms.

Remark 2 Since the Hill function mapping the drug effect to the *BIS*(t) output is nonlinear, the feedback signal is taken from the linear output $Y_p(t)$ which is not directly measurable. Therefore, its estimate $\hat{Y}_p(t)$ is employed in the feedback loop and the control law.

substituting $\hat{Y}_p(t)$ from (18) into (22), we obtain

$$\frac{\hat{Y}_p(t)}{r(t)} = \frac{G_p(s)\,K_r^*}{1 - K_1^{*T}\frac{\alpha(s)}{\Lambda(s)} - G_p(s)K_2^{*T}\frac{\alpha(s)}{\Lambda(s)} - G_p(s)K_e^*}, \tag{25}$$

expanding the denominator of (25) yields

$$1 - K_1^{*T}\frac{\alpha(s)}{\Lambda(s)} - \frac{k_p N(s)}{D(s)}K_2^{*T}\frac{\alpha(s)}{\Lambda(s)} - \frac{k_p N(s)}{D(s)}K_e^*, \tag{26}$$

by multiplying the numerator and denominator of (25) by $\Lambda(s)D(s)$, and defining

$$D_0(s) = \Lambda(s)D(s)\left(1 - K_1^{*T}\frac{\alpha(s)}{\Lambda(s)} - \frac{k_p N(s)}{D(s)}K_2^{*T}\frac{\alpha(s)}{\Lambda(s)} - \frac{k_p N(s)}{D(s)}K_e^*\right), \tag{27}$$

equation (25) can be written as

$$\frac{\hat{Y}_p(t)}{r(t)} = \frac{k_p N(s)\Lambda(s)K_r^*}{D_0(s)}. \tag{28}$$

Now, according to the matching condition that $\hat{Y}_p(t)$ should track $y_m(t)$ and (21), we need to have

$$\frac{k_p N(s)\Lambda(s)K_r^*}{D_0(s)} = \frac{1}{D_m(s)}, \tag{29}$$

by choosing $K_r^* = \frac{1}{k_p}$, it is simplified to

$$D_0(s) = D_m(s)N(s)\Lambda(s), \tag{30}$$

consequently, from (27) and (30), the polynomial matching condition which is used in error equation parametrization is obtained as

$$K_1^{*T}\alpha(s)D(s) + k_pN(s)[K_2^{*T}\alpha(s) + K_e^*\Lambda(s)] = \Lambda(s)D(s) - D_m(s)N(s)\Lambda(s). \tag{31}$$

We now reintroduce the input delay in the PK/PD model. The closed-loop plant (18), with delay can be expressed as

$$Y_p(t) = G_p(s)u(t) + G_p(s)a_\tau^{*T}x(t - \tau(t)), \tag{32}$$

operating both sides of (31) on $\hat{Y}_p(t)$ and using $G_p(s)$ from (18) and (32), we have

$$K_1^{*T}F(s)k_pN(s)u(t) + K_1^{*T}F(s)k_pN(s)a_\tau^{*T}x(t - \tau(t)) + K_2^{*T}F(s)k_pN(s)\hat{Y}_p(t) + K_e^*k_pN(s)\hat{Y}_p(t) = k_pN(s)u(t) + k_pN(s)a_\tau^{*T}x(t - \tau(t)) - N(s)D_m(s)\hat{Y}_p(t), \tag{33}$$

dividing both sides by $N(s)D_m(s)$ and using (23), the plant output can be written as

$$\hat{Y}_p(t) = \frac{k_p}{D_m(s)}[u(t) - K_e^*\hat{Y}_p(t) - K_1^{*T}\omega_1(t) - K_2^{*T}\omega_2(t) + a_\tau^{*T}x(t - \tau(t)) - K_1^{*T}F(s)\, a_\tau^{*T}x(t - \tau(t))]. \tag{34}$$

Using the reference model (21), the tracking error

$$e(t) = \hat{Y}_p(t) - y_m(t), \tag{35}$$

is finally obtained as

$$e(t) = \frac{k_p}{D_m(s)}[u(t) - K_e^*\hat{Y}_p(t) - K_1^{*T}\omega_1(t) - K_2^{*T}\omega_2(t) - K_r^*r(t) + a_\tau^{*T}x(t - \tau(t)) - K_1^{*T}F(s)a_\tau^{*T}x(t - \tau(t))]. \tag{36}$$

To avoid unnecessary complexity in the subsequent stability analysis, the tracking error dynamics are first rewritten into a convenient parametric form. Therefore, to derive an appropriate parametrization of the error dynamics, the system equations are defined as follows

$$z(t) = K_1^{*T}F(s)[a_\tau^{*T}x(t - \tau(t))] = K_z^{*T}z_x(t), \tag{37}$$

where

$$K_z^{*T} = [\, K_1^{*T}a_\tau^{*T} \quad K_1^{*2T}a_\tau^{*T} \quad K_1^{*3T}a_\tau^{*T}], \tag{38}$$

$$z_x(t) = F_4(s)[x(t - \tau(t))],$$

$$F_4(s) = \frac{[I_{4\times4}s^2,\, I_{4\times4}s,\, I_{4\times4}]}{\Lambda(s)} \in \Re^{12\times4}.$$

By decomposing $z_x(t)$ into two components we have

$$z_x(t) = z_e(t) + z_m(t), \tag{39}$$

$$z_e(t) = F_4(s)e_x(t - \tau(t)),$$

$$z_m(t) = F_4(s)x_m(t - \tau(t)),$$

$e_x(t - \tau(t)) = x(t - \tau(t)) - x_m(t - \tau(t))$.

where $x_m(t) \in \Re^4$ denotes the state of the reference model realization with triple (A_m, B_m, c_m). Using (37) and (39) the error dynamics in (36) can be expressed in the following equivalent form

$$e(t) = \frac{k_p}{D_m(s)}[u(t) - K^{*T}\omega(t)] - \frac{k_p}{D_m(s)}[K_m^{*T}\omega_m(t) - a_\tau^{*T}e_x(t - \tau(t)) + K_z^{*T}z_e(t)], \tag{40}$$

where,

$$K^* = [K_1^{*T} \quad K_2^{*T} \quad K_e^* \quad K_r^*]^T, \tag{41}$$

$$\omega(t) = [\omega_1{}^T(t) \quad \omega_2{}^T(t) \quad e(t) \quad r(t)]^T,$$

$$K_m^* = [K_e^* c_m \quad -a_\tau^{*T} \quad K_z^{*T}]^T,$$

$$\omega_m(t) = [x_m(t) \quad x_m(t - \tau(t)) \quad z_m^T(t)]^T.$$

Since the reference model $W_m(s)$ has relative degree of two, it is not strictly positive real (SPR). Therefore, following the standard approach in relative-degree-two MRAC [38], we introduce a first-order stable filter

$$Z(s) = s + p_0, \qquad p_0 > 0, \tag{42}$$

such that $W_m(s)Z(s)$ becomes strictly positive real. Using the identity

$$(s + p_0)(s + p_0)^{-1} = 1, \tag{43}$$

the error equation (40) can be rewritten as

$$e(t) = \frac{k_p(s + p_0)}{D_m(s)}[u_f(t) - K^{*T}\varphi(t)] - \frac{k_p}{D_m(s)}[K_m^{*T}\omega_m(t) - a_\tau^{*T}e_x(t - \tau(t)) + K_z^{*T}z_e(t)], \tag{44}$$

where

$$u_f(t) = \frac{1}{s + p_0}u(t), \qquad \varphi(t) = \frac{1}{Z(s)}\omega(t) = \frac{1}{s + p_0}\omega(t). \tag{45}$$

Based on this tracking error, the control law is selected as

$$u_f(t) = K^T(t)\varphi(t) - K_I \text{sgn}(e(t)) \int_0^t |e(t)|dt, \tag{46}$$

where $K(t)$ is the estimation of the controller parameter vector K^*, $K_I > 0$ is a constant design parameter introduced to enhance robustness against unknown delays and external disturbances, and sgn($e(t)$) denotes the standard sign function.

According to (45), the actual control input $u(t)$ applied to the delayed PK/PD plant (16) is obtained as

$$u(t) = (s + p_0)u_f(t) = (s + p_0)[K^T\varphi(t) - K_I \text{sgn}(e(t)) \int_0^t |e(t)|dt] = K^T\omega(t) + \dot{K}^T\varphi(t) - K_I e(t) - K_I p_0 \text{sgn}(e(t)) \int_0^t |e(t)|dt, \tag{47}$$

Remark 3 The control law (47) consists of two parts. The first part, $K^T\omega(t) + \dot{K}^T\varphi(t)$, corresponds to the controller structure introduced in [38] for output-feedback control of systems, specifically for an MRAC controller designed for a plant with relative degree two, while the second part, $K_I e(t)$ -

$K_I p_0 \text{sgn}(e(t)) \int_0^t |e(t)|dt$, is employed to achieve the necessary robustness against unknown delays in the system. From a practical implementation perspective, the proposed control law is realizable, since the parameter update law $\dot{K}(t)$ is obtained directly from the adaptation laws, and the BIS signal is measurable. However, due to the nonlinearity of the Hill function, the estimated linear output $\hat{Y}_p(t)$, obtained via the inverse Hill transformation, is used in the feedback loop.

Substituting $u_f(t)$ into (44) yields

$$e(t) = \frac{k_p(s + p_0)}{D_m(s)} [\tilde{K}^T(t)\varphi(t) - K_I \text{sgn}(e(t)) \int_0^t |e(t)|dt] - \frac{k_p}{D_m(s)} [K_m^{*T}\omega_m(t) - a_\tau^{*T} e_x(t - \tau(t)) + K_z^{*T} z_e(t)], \quad (48)$$

where $\tilde{K}^T(t) = K(t) - K^*(t)$ is the parameter estimation error. Now, we write the tracking-error dynamics (48) in an equivalent state-space form. The augmented state vector $\hat{x} = [x^T \quad \omega_1^T \quad \omega_2^T]^T$ is defined. Let $\hat{e}(t) \triangleq \hat{x}(t) - \hat{x}_m(t)$ where $\hat{x}_m(t)$ is the state of a non-minimal realization $\hat{c}(sI - \hat{A})^{-1} b_1 K_r^*$ of $W_m(s)$. Then we obtain state space representation

$$\dot{\hat{e}}(t) = \hat{A}\hat{e}(t) + \hat{b}(s + p_0)(\tilde{K}^T(t)\varphi(t) - K_I \text{sgn}(e(t)) \int_0^t |e(t)|dt) - \hat{b}[K_m^{*T}\omega_m(t) - a_d^{*T} L^T e_x(t - \tau(t)) + K_z^{*T} C_e z_e(t)], \quad (49)$$

$$\dot{\hat{z}}_e(t) = A_e \hat{z}_e(t) + B_e\, e_x(t - \tau(t)),$$

$$z_e(t) = C_e \hat{z}_e(t),$$

$$e(t) = \hat{c}\hat{e}(t),$$

for (48), where $L = [I_{4\times4} \quad 0_{4\times3} \quad 0_{4\times3}]^T$ and the triple (A_e, B_e, C_e) constitutes a minimal state-space realization of the stable transfer matrix $F_4(s)$.

To facilitate the Lyapunov analysis for the relative-degree-two case, a suitable coordinate transformation is introduced to rewrite the error dynamics in a form compatible with the SPR framework. Specifically, we define the transformed error variable as

$$\bar{e}(t) \triangleq \hat{e}(t) - \hat{b}(\tilde{K}^T(t)\varphi(t) - K_I \text{sgn}(e(t)) \int_0^t |e(t)|dt). \quad (50)$$

This transformation eliminates the direct dependence of the error dynamics on the filtered regressor term and allows the control input to enter the system in a strictly proper manner.

Substituting (50) into the error dynamics derived in (49), the closed-loop error system can be rewritten as

$$\dot{\bar{e}}(t) = \hat{A}\bar{e}(t) + b_1(\tilde{K}^T(t)\varphi(t) - K_I \text{sgn}(e(t)) \int_0^t |e(t)|dt) - b_1[\theta_m^{*T}\omega_m + \theta_d^{*T} L^T e_x(t - \tau(t)) + \theta_z^{*T} C_e \hat{z}_e(t)], \quad (51)$$

$$\dot{\hat{z}}_e(t) = A_e \hat{z}_e(t) + B_e e_x(t - \tau(t)),$$

$$z_e(t) = C_e \hat{z}_e(t),$$

$$e(t) = \hat{c}\bar{e}(t).$$

where $b_1 = \hat{A}\hat{b} + \hat{b}p_0$, $\theta_m^{*T} = b_1^{-1}\hat{b}K_m^{*T}$, $\theta_d^{*T} = b_1^{-1}\hat{b}K_d^{*T}$, $\theta_z^{*T} = b_1^{-1}\hat{b}K_z^{*T}$.

This transformation yields an equivalent error system in which the transfer function from the adaptive control input to the tracking error is given by $W_m(s)Z(s)$, which is strictly positive real. This property is

essential for the subsequent Lyapunov-Krasovskii stability analysis. The SPR property of the transformed error system allows the use of the Meyer–Kalman–Yakubovich (MKY) lemma, ensuring the existence of a quadratic Lyapunov function. Since $\hat{c}(sI - \widehat{A})^{-1} b_1 K_r^* = \hat{c}(sI - \widehat{A})^{-1} \hat{b} K_r^* (s + p_0) = W_m(s)(s + p_0)$ is SPR, and based on the MKY lemma, for any positive definite symmetric matrix $L_c = L_c{}^T > 0$, there exists a positive definite symmetric matrix $P = P^T > 0$, a scalar $\nu > 0$, and a vector q such that

$$\begin{aligned} &\widehat{A}^T P + P \widehat{A} = - qq^T - \nu L_c, \\ &Pb_1 K_r^* = \hat{c}^T. \end{aligned} \tag{52}$$

Since A_e is stable, there exist symmetric positive definite matrices $P_z = P_z{}^T > 0$ and $Q_z = Q_z{}^T > 0$ such that

$$A_e{}^T P_z + P_z A_e = -Q_z \, . \tag{53}$$

Now the theorem for the designed controller can be stated. The following derivation establishes the stability of the transformed delayed error dynamics and guarantees asymptotic convergence of the tracking error.

Theorem 1 Consider PK/PD model (16) and reference model (21), therefore, for any positive scalar γ and any positive definite matrix $\Gamma_1 = \Gamma_1{}^T > 0$, the control input defined in (47), together with the adaptive law, yields

$$\begin{aligned} &\dot{K}(t) = - \operatorname{sgn}(\rho^*) \Gamma_1 e(t) \varphi(t), \\ &K_I = \gamma \operatorname{sgn}(\rho^*), \end{aligned} \tag{54}$$

which guarantees bounded closed-loop signals and asymptotic convergence of the tracking error $e(t)$ to zero.

Proof The stability of the proposed scheme is established by considering the following Lyapunov–Krasovskii functional candidate

$$V(t) = \bar{e}^T(t) P \bar{e}(t) + \hat{z}_e{}^T(t) P_z \hat{z}_e(t) + \int_{t - \tau(t)}^{0} e_x^T(s) \nu L_c e_x(s) ds + \left(\widetilde{K}(t) - \overline{K}_1\right)^T \Gamma_1{}^{-1} \left(\widetilde{K}(t) - \overline{K}_1\right) \left|\rho^*\right|. \tag{55}$$

The vector $\overline{K}_1$ is described as follows

$$\overline{K}_1 = - \frac{r_1}{2} (s + p_0) \left[\rho^*, \, 0, \, \ldots, \, 0\right]^T, \tag{56}$$

with $r_1 > 0$ being an arbitrary constant scalar. With this definition we have

$$2 \overline{K}_1 \varphi(t) = 2 \overline{K}_1{}^T \times \frac{1}{(s + p_0)} \omega(t) = -r_1 \rho^* e(t) = -r_1 \bar{e}^T(t) P b_1. \tag{57}$$

Using the adaptation law (54) and applying (52) and (53), the time derivative of $V(t)$ with respect to (51) is given by

$$\begin{aligned} \dot{V}(t) = &-\bar{e}^T(t) qq^T \bar{e}(t) - \nu \bar{e}^T(t) L_c \bar{e}(t) - \nu (1 - \dot{\tau}(t)) e_x^T(t - \tau(t)) L_c e_x(t - \tau(t)) - r_1 \bar{e}^T(t) P b_1 b_1{}^T P \bar{e}(t) - \\ &\hat{z}_e{}^T(t) Q_z \hat{z}_e(t) - 2 \bar{e}^T(t) P b_1 \theta_z^{*T} e_x(t - \tau(t)) - 2 \bar{e}^T(t) P b_1 \theta_z^{*T} C_e \hat{z}_e + 2 \hat{z}_e{}^T P_z B_e e_x(t - \tau(t)) - 2 \bar{e}^T(t) P b_1 \theta_m^{*T} \omega_m. \end{aligned} \tag{58}$$

Since D_m(s) and $F_4(s)$ are stable and the reference input $r(t)$ is bounded, the corresponding reference signals $x_m(t)$, $x_m(t - \tau(t))$ and $z_m(t)$ remain bounded. Therefore, a finite constant ω_{m1}^* exists such that the $\|\omega_m\| \leq \omega_{m1}^*$. Consequently, the last term of (58) can be bounded as

$$-2\bar{e}^T P b_1 \theta_m^{*T} \omega_{m1} \le 2\left|\bar{e}^T P b_1 K_0{}^*\right|\left|\rho^*\right|\left\|\theta_m^{*T}\right\|\omega_{m1}^*. \tag{59}$$

By selecting $\eta_1^* = \left\|\theta_m^{*T}\right\|\omega_{m1}^*$, it can be written as

$$-2\bar{e}^T P b_1 \theta_m^{*T} \omega_m \le 2\eta_1^*\left|\rho^*\right||e(t)|. \tag{60}$$

According to the following inequality

$$\pm x^T y \le x^T S x + y^T S^{-1} y, \tag{61}$$

where S is a positive definite matrix introduced for inequality bounding, the following definitions can be written for the sixth, seventh, and eighth terms of (58)

$$-2\bar{e}^T(t) P b_1 \theta_d^{*T} e_x(t - \tau(t)) \le \bar{e}^T(t) P b_1 \Psi_1 b_1 P \bar{e}(t) + e_x^T(t - \tau(t)) S e_x(t - \tau(t)), \tag{62}$$

$$-2\bar{e}^T(t) P b_1 \theta_z^{*T} C_e \hat{z}_e \le \bar{e}^T(t) P b_1 \Psi_2 b_1{}^T P \bar{e}(t) + z_e^T S \hat{z}_e,$$

$$2\hat{z}_e^T P_z B_e e_x(t - \tau(t)) \le \hat{z}_e^T \Psi_3 \hat{z}_e + e_x^T(t - \tau(t)) S\, e_x(t - \tau(t)),$$

where,

$$\Psi_1 = \theta_d^{*T} S^{-1} \theta_d^*, \tag{63}$$

$$\Psi_2 = \theta_z^{*T} C_e S^{-1} C_e^T \theta_z^*,$$

$$\Psi_3 = P_z B_e S^{-1} B_e^T P_e^T.$$

Using (60) and (61), and incorporating the coefficient K_I from (54), the following inequality is obtained

$$\dot{V}(t) \le -\bar{e}^T(t) q q^T \bar{e}(t) - v\bar{e}^T(t) L_c \bar{e}(t) - e_x^T(t - \tau(t))(v\tau^* L_c - 2S) e_x(t - \tau(t)) - \bar{e}^T(t) P b_1 (r_1 - \Psi_1 - \Psi_2) b_I^T P \bar{e}(t) - \hat{z}_e^T(t)(Q_z - \Psi_3 - S)\hat{z}_e(t), \tag{64}$$

where $\tau^* = 1 - \bar{\tau}$. If the design parameters L_c, r_1, and Q_z satisfy

$$\lambda_{min}(vL_c) > \lambda_{min}(2S), \tag{65}$$

$$r_1 > \lambda_{max}(\Psi_3 + S),$$

$$\lambda_{min}(Q_z) > \lambda_{max}(\Psi_3 + S),$$

then, $\dot{V}(t) \le 0$. Consequently, all closed-loop signals, including $e(t)$, $\hat{e}(t)$, and $\tilde{K}(t)$, remain bounded. Moreover, from (64), we obtain $e \in L_2 \cap L_\infty$ and $\dot{e} \in L_\infty$. By Barbalat's lemma, this implies

$$\lim_{t \to \infty} \mathrm{e(t)} = 0\ . \tag{66}$$

Having established the theoretical framework and derived the MRAC control law, the following section presents the simulation results to validate its effectiveness.

4. Results and discussion

The performance of the proposed control approach is assessed through simulation studies conducted under clinically relevant conditions. Each simulation covers a 35-minute interval, including both induction and

maintenance phases of anesthesia. During the induction phase, the control objective is formulated as a tracking problem, where the reference signal $r(t)$ is defined as a step transition from the initial BIS level E_0 to a target value of 50. This phase aimed to evaluate the system's ability to rapidly and accurately reach the desired depth of anesthesia. In the design, analysis, and assessment of the control system, a constant dosing ratio (M) of 2:1 (remifentanil to propofol) was adopted. Although this proportion may differ depending on the specific surgical procedure, it represents the most commonly used setting, as it follows the infusion scheme outlined in [28]. In the subsequent maintenance phase, the controller's disturbance rejection capability was tested by introducing simulated surgical stimulation. To emulate this effect, a disturbance signal $d(t)$ in the form of a double-step input was applied to the BIS output. Specifically, a positive step of magnitude 10 was introduced at the 15-minute mark, followed by a negative step of equal magnitude at minute 25, effectively returning $d(t)$ to zero and simulating the end of the stimulus. Fig. 3 depicts the disturbance signal.

For propofol parameters, the virtual patient population reported in [41], generated from realistically distributed biometric variables, was utilized to evaluate inter-patient variability. No new patient data were collected or generated in the present study. For remifentanil, model parameters were randomly generated from normal distributions based on the pharmacodynamic values reported in the literature [42]. It is important to emphasize that these parameters are only used for plant simulation and are not used in control law. The demographic characteristics of these patients, along with the mean values of all features, are provided in Table II.

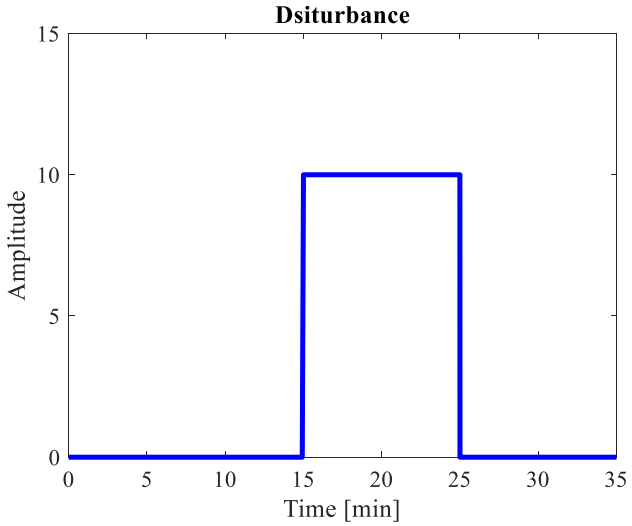


Fig. 3. Disturbance signal.

Table II. Patient characteristics [41,42].

PATIENT	GENDER	AGE	WEIGHT	HEIGHT	E_0	E_{MAX}	$X_{e50,p}$	$X_{e50,r}$	β	γ
1	F	40	54	163	98.80	94.10	6.33	12.5	2.00	2.24
2	F	36	50	163	98.60	86.00	6.76	12.7	1.50	4.29
3	F	28	52	164	91.20	80.70	8.44	7.1	1.00	4.1
4	F	50	83	163	95.90	102.00	6.44	11.1	1.30	2.18

5	M	28	60	164	94.70	85.30	4.93	12.5	1.20	2.46
6	F	43	59	163	90.20	147.00	12.10	12.7	1.30	2.42
7	M	37	75	187	92.00	104.00	8.02	10.5	0.80	2.10
8	F	38	80	174	95.50	76.40	6.56	9.9	1.00	4.12
9	F	41	70	170	89.20	63.80	6.15	11.6	1.70	6.89
10	F	37	58	167	83.10	151.00	13.70	16.7	1.90	1.65
11	M	42	78	179	91.80	77.90	4.82	14.0	1.20	1.85
12	F	34	58	172	96.20	90.80	4.95	8.8	0.90	1.84
13	F	38	65	169	93.1	96.58	7.42	10.5	1.00	3.00

In this study, the stable reference model with relative degree two is chosen ($W_m(s) = \frac{1}{(s+1)^2}$) and p_0 is selected such that $W_m(s)(s + p_0)$ is strictly positive real ($p_0 = 1$). Based on the selected reference model ($W_m(s)$), the reference model matrices are obtained as $A_m = \begin{bmatrix} 0 & 1 \\ -1 & -2 \end{bmatrix}$, $B_m = \begin{bmatrix} 0 \\ 1 \end{bmatrix}$, and $c_m{}^T = [1 \quad 0]$. Moreover, $\Lambda(s)$ is chosen as

$$\Lambda(s) = (s + 1)^3. \tag{67}$$

According to (10), the normalized remifentanil effect is approximated as proportional to the normalized propofol effect. To obtain a representative value of μ, the dynamic relation between the two drug pathways was simplified using a steady-state approximation and scaled according to the corresponding 50% effective concentrations. Therefore,

$$\mu \approx M\frac{X_{e_{50},p}}{X_{e_{50},r}}. \tag{68}$$

Using the average patient parameters listed in Table II and the fixed co-administration ratio $M = 2$, the resulting proportional coefficient was selected as $\mu \approx 1.25$.

4.1 Performance assessment

The performance of the closed-loop system is evaluated using clinically meaningful metrics for both induction and maintenance phases, as described in [43]. The induction-phase performance metrics are summarized as follows:

1. **BIS-NADIR**: The minimum BIS value observed during the induction phase.
2. **TT** (Time to Target BIS 50): the elapsed time required for the BIS value to reach 50 for the first time. In manual practice, this typically falls within the range of 120–360 seconds.
3. **ST10** (Settling Time to 10% band): In this study, settling time refers to the time necessary for the BIS to enter and stay within the target interval of [45, 55]. For manual administration, this time typically falls between 120 and 300 seconds.

The performance metrics for the maintenance phase are defined as follows:

1. **BIS-NADIRn**: The maximum measured BIS value observed following the application of a negative disturbance pulse.
2. **BIS-NADIRp**: The minimum measured BIS value observed following the application of a positive disturbance pulse.
3. **RTPD** (Recovery Time from Positive Disturbance): The BIS response time to return to the interval [45, 55] following the occurrence of a positive disturbance.
4. **RTND** (Recovery Time from Negative Disturbance): The BIS response time to return to the interval [45, 55] following the occurrence of a negative disturbance.
5. **BIS > 60**: The total duration over which the measured BIS value remains above 60.
6. **BIS < 40**: The total duration over which the measured BIS value remains below 40.

For a more accurate evaluation of the controller, performance indices such as performance error and standard deviation were employed [44].

- **Performance Error (PE)**

Performance error is a percentage-based metric that quantifies the deviation from the setpoint at each time step. It is calculated as

$$\mathrm{PE}(t) = \frac{BIS_m(t) - BIS_{reference}(t)}{BIS_{reference}(t)} \times 100\%, \tag{69}$$

where $BIS_{reference}(t)$ is the reference BIS, which is set to 50.

- **Standard Deviation**

Standard deviation is a statistical indicator that reflects the dispersion of data points relative to their mean value. In other words, it shows how far the data points deviate from the mean and is calculated as

$$\sigma = \sqrt{\frac{(\bar{x} - x_1)^2 + (\bar{x} - x_2)^2 + \ \ldots \ + (\bar{x} - x_n)^2}{n}}, \tag{70}$$

where σ is the standard deviation, $\bar{x}$ denotes the mean of the data, and n represents the number of data points.

In the proposed simulations, the control outputs are interpreted as clinically relevant infusion rates after appropriate unit mapping for each drug. Therefore, propofol infusion is expressed in mg/kg/min, while remifentanil administration is represented in µg/kg/min. In clinical practice, propofol is commonly administered with an induction infusion of approximately 1–2 mg/kg/min, followed by a maintenance rate in the range of 0.05–0.15 mg/kg/min (50–150 µg/kg/min). Remifentanil is typically delivered with an initial dose around 0.5–1 µg/kg/min and maintained within 0.1–0.4 µg/kg/min. These ranges are consistent with standard clinical anesthesia practice and help avoid both overdosing and insufficient anesthesia [45].

The induction phase responses of the BIS signal for all 12 patients are illustrated in Fig. 4, while the corresponding performance indices are summarized in Table III. As shown in Fig. 4, the proposed adaptive controller successfully drives the BIS value from its initial level E_0 to the desired target of 50 in all cases,

despite significant inter-patient variability. The TT values indicate rapid induction without aggressive control action. Moreover, BIS-NADIR remained above 40 in all patients, indicating avoidance of excessive anesthetic depth. The ST10 results further confirm stable convergence of the BIS signal after transient deviations. Although some variability in TT and ST10 is observed across patients, this behavior reflects differences in patient-specific PK/PD characteristics rather than instability, demonstrating consistent performance under inter-patient variability.

The maintenance phase performance of the proposed controller in the presence of surgical disturbances is presented in Fig. 5, with quantitative results reported in Table IV. The applied double-step disturbances produced temporary BIS deviations; however, the controller rapidly restored the BIS signal to the target range in all patients. The short RTPD and RTND values reported in Table IV further confirm effective disturbance compensation. The BIS-NADIRp and BIS-NADIRn values remain close to the reference value of 50, confirming that the controller avoids both excessive anesthesia depth and insufficient sedation during the maintenance phase. The low standard deviation of the maintenance-phase performance metrics further confirms the robustness and consistency of the controller under inter-patient variability and time-varying disturbances.

Figures 6 and 7 illustrate the drug delivery profiles for propofol and remifentanil throughout the induction and maintenance stages in all patients. During induction (Fig. 6), the controller initially increases the drug infusion rates to rapidly achieve the desired anesthesia level, followed by a gradual reduction as the BIS approaches the target, indicating smooth and well-regulated control behavior. During the maintenance phase (Fig. 7), moderate adjustments in the infusion rates are observed in response to the applied disturbances, demonstrating effective disturbance rejection. In all cases, the infusion profiles remained within acceptable clinical limits. The simplified inverse Hill reconstruction introduced in Section 3 enabled estimation of the linearized drug effect directly from BIS measurement without requiring a fully nonlinear multi-input estimator. Despite this simplification, stable BIS regulation was achieved across all simulated patients.

Figures 8 and 9 present the mean delivery rates of propofol and remifentanil and the corresponding average BIS responses over the entire anesthesia period, respectively. As shown in Fig. 9, inclusion of the integral term improved BIS tracking performance, particularly during disturbance intervals, while maintaining smooth infusion profiles. In the absence of the integral term, larger deviations from the reference BIS value are observed, indicating reduced compensation of delayed dynamics. Meanwhile, Fig. 8 shows that this improved performance is achieved without excessive drug administration, as the average infusion rates remain smooth and within safe infusion limits. These results demonstrate that the proposed control structure effectively compensates for time-varying delays while preserving safety and practical feasibility.

Finally, Fig. 10 shows the performance error for all patients during anesthesia. The error rapidly converges to zero after induction and remains bounded within a narrow range, even in the presence of disturbances, indicating accurate tracking and robust compensation of time-varying delays across patients.

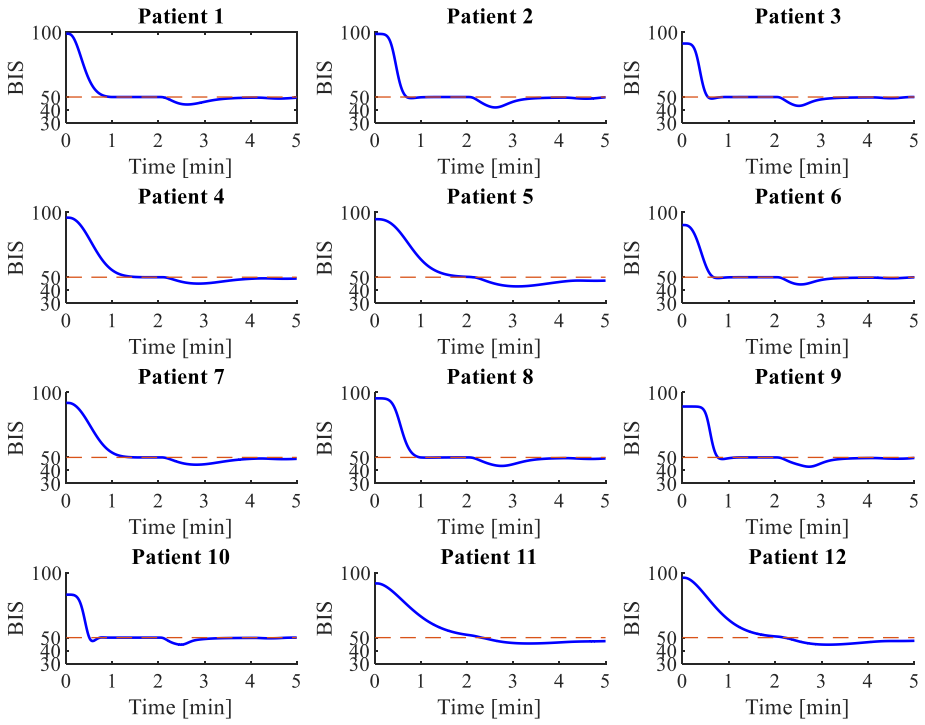


Fig. 4. Simulation results of $BIS_m(t)$ of the proposed model reference adaptive controller with the 12 patients in the induction phase.

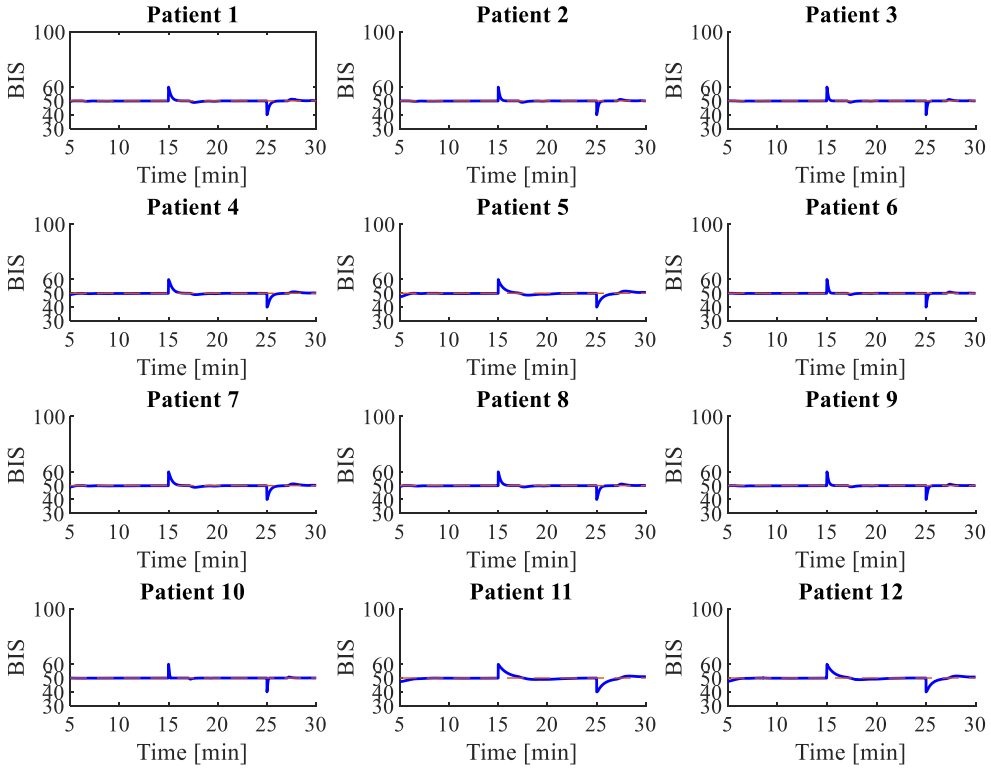


Fig. 5. Simulation results of $BIS_m(t)$ of the proposed model reference adaptive controller with the 12 patients in the maintenance phase.

Table III. Evaluation of the induction phase of anesthesia using a model reference adapive controller for delayed systems characteristics.

Patient	TT [s]	BIS-NADIR	ST10 [s]
1	140	44.10	279
2	104	41.55	250
3	105	42.50	248
4	155	45.38	141
5	128	44.11	240
6	120	43.58	256
7	120	42.15	273
8	180	44.94	305
9	185	44.39	350
10	162	42.87	360
11	150	44.56	288
12	193	45.44	166
Mean	145.17	43.80	263
Standard Deviation	31.13	1.28	63.96

Table IV. Evaluation of the maintenance phase of anesthesia using a model reference adapive controller for delayed systems characteristics.

Patient	RTND [min]	RTPD [min]	BIS-NADIRn	BIS-NADIRp	BIS>60	BIS<40
1	0.65	0.75	51.30	48.80	0	0
2	0.36	0.34	51.55	48.87	0	0
3	0.34	0.31	51.51	48.58	0	0
4	0.68	0.67	51.02	49.00	0	0
5	0.37	0.36	51.30	48.62	0	0
6	0.47	0.43	51.42	48.86	0	0
7	0.41	0.34	51.33	48.90	0	0
8	0.73	0.79	51.23	48.64	0	0
9	1.08	1.04	51.53	48.68	0	0
10	0.84	0.79	51.59	48.56	0	0
11	0.60	0.64	51.30	48.82	0	0
12	1.28	1.22	51.56	48.80	0	0
Mean	0.65	0.64	51.38	48.75	0	0
Standard Deviation	0.31	0.30	0.14	0.10	0	0

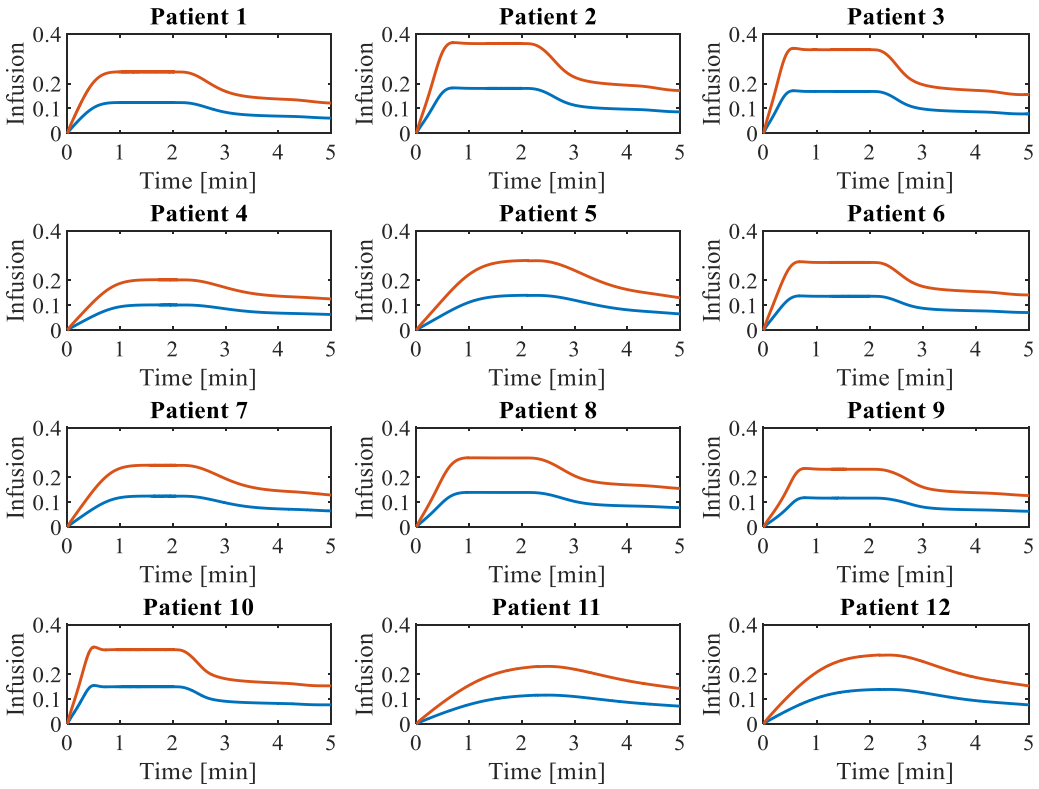


Fig. 6. Propofol (blue curve mg/kg/min) and Remifentanil (red curve µg/kg/min) infusion for the 12 patients during the induction phase. Typical manual administration rates for propofol and remifentanil are 1–2 mg/kg/min and 0.5–1 µg/kg/min during induction, respectively.

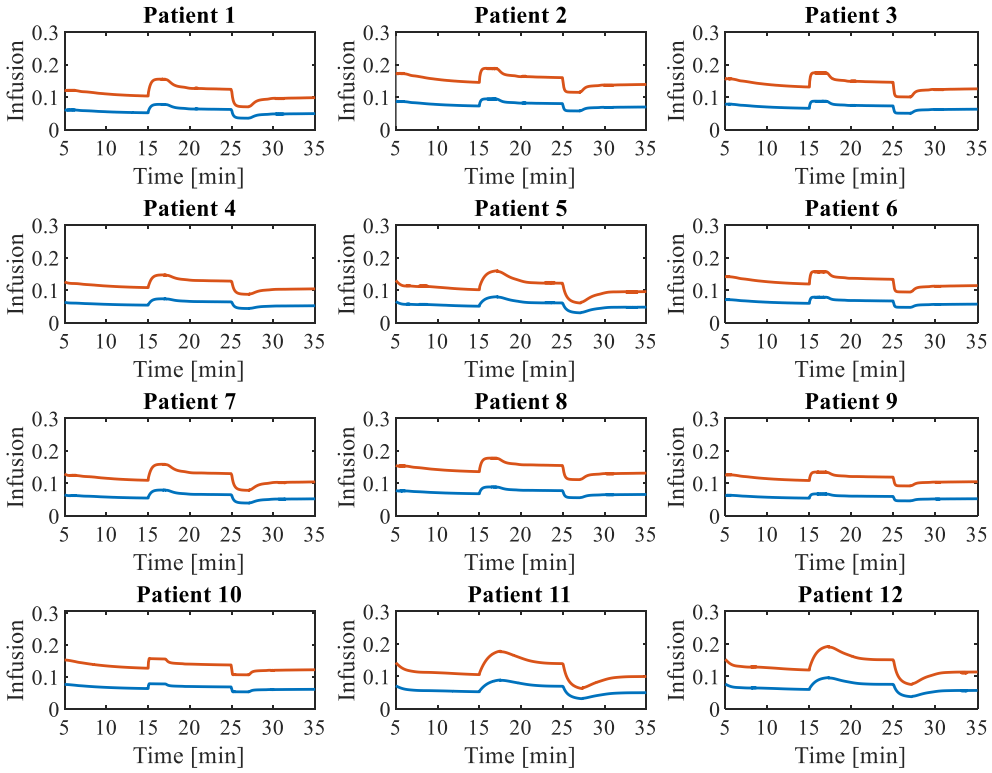


Fig. 7. Propofol (blue curve mg/kg/min) and Remifentanil (red curve µg/kg/min) infusion for the 12 patients during the maintenance phase. Typical manual administration ranges during maintenance phase are 0.05–0.15 mg/kg/min for propofol and 0.1–0.4 µg/kg/min for remifentanil.

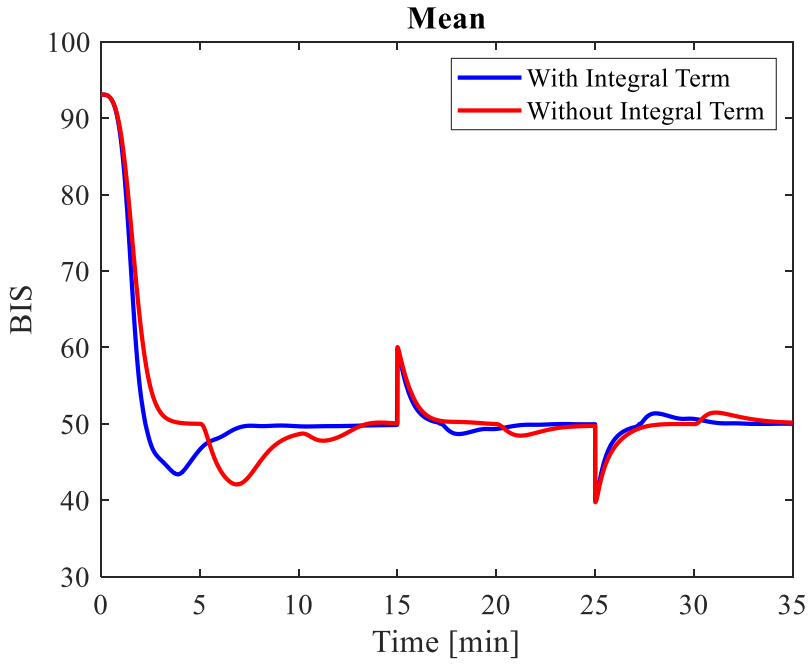


Fig. 8. The average $BIS_m(t)$ of 12 patients are shown, comparing the delayed system without integral term (red curve) with the proposed control structure with integral term for the delayed system (blue curve).

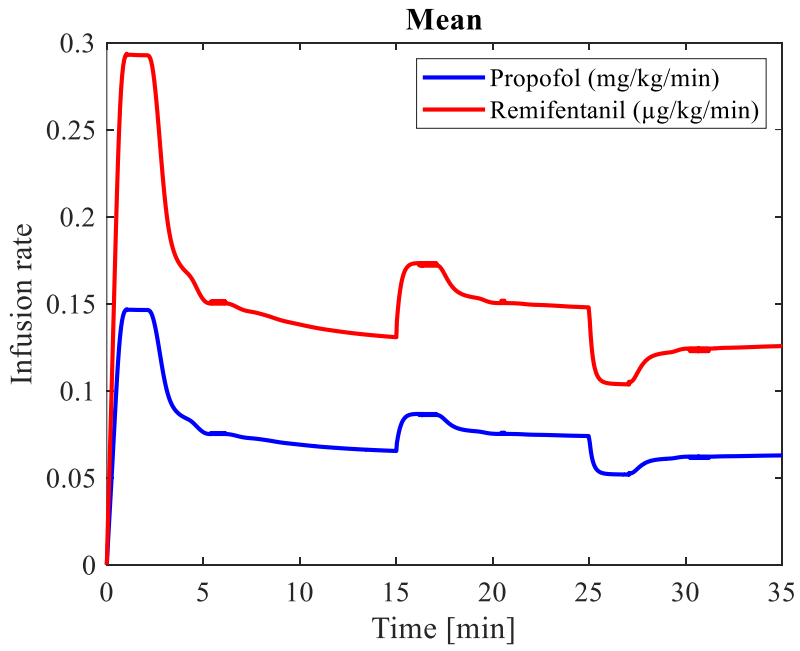


Fig. 9. Mean infusion rates of propofol (blue) and remifentanil (red) for 12 patients under the proposed MRAC scheme with time delay compensation. For reference, typical infusion rates during induction are 1–2 mg/kg/min for propofol and 0.5–1 µg/kg/min for remifentanil, whereas during the maintenance phase they are 0.05–0.15 mg/kg/min and 0.1–0.4 µg/kg/min, respectively.

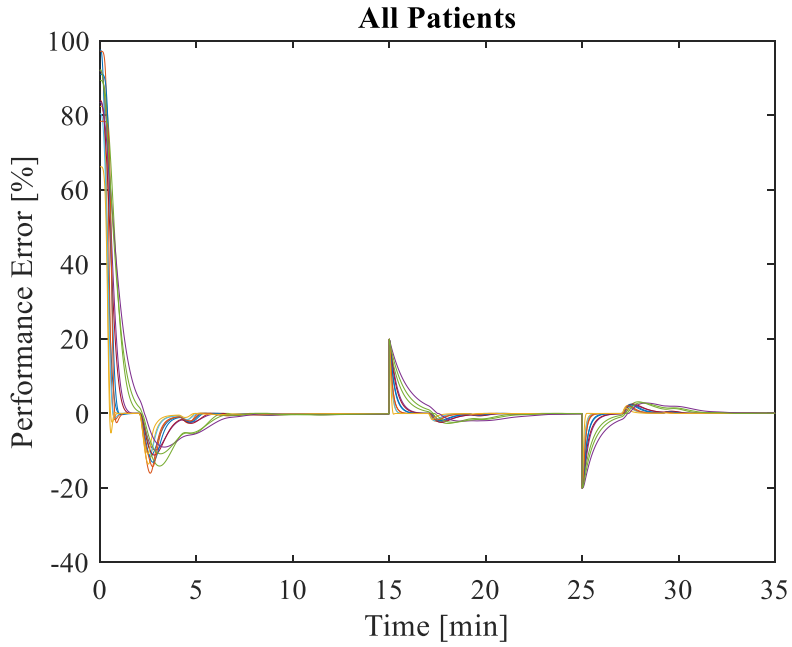


Fig. 10. Performance error of the 12 patients during anesthesia using a model reference adaptive controller (MRAC) designed for systems with time delay.

4.2 Comparison with existing control strategies

Table V presents a comparative summary of the proposed Model Reference Adaptive Controller (MRAC) against other advanced control strategies previously reported in the literature.

Table V. Comparison of the proposed MRAC with other control strategies.

Study	Control Strategy	Drug administration	Inverse Hill-based feedback	Automatic parameter update	Explicit Delay handling	Need for patient specific parameters
Navarro-Guerrero et al. (2017) [30]	Fractional-Order MRAC	Propofol	✗	✓	✓	✗
Merigo et al. (2019) [43]	Optimized PID	Propofol and Remifentanil	✗	✗	✓	✓
Pawłowski et al. (2022) [28]	Nonlinear MPC	Propofol and Remifentanil	✓	✗	✗	✓
Pawłowski et al. (2022) [46]	Even-based MPC	Propofol and Remifentanil	✓	✗	✗	✓
Proposed Method	MRAC	Propofol and Remifentanil	✓	✓	✓	✗

In contrast to the fractional-order MRAC proposed in [30], which employs a fractional model directly on the BIS signal and considers only propofol infusion, the proposed approach is developed on an explicit PK/PD framework and is designed for jointly administering propofol and remifentanil. In this study, the nonlinear Hill relationship between drug effect and BIS is explicitly compensated using an inverse Hill transformation, allowing the adaptive controller to operate on an estimated linear effect-site output rather than implicitly absorbing the nonlinearity into the system dynamics. Moreover, while the robustness to delays in [30] relies mainly on the memory effect of fractional-order dynamics, the proposed method explicitly incorporates time-varying physiological delays into both the control design and the Lyapunov–Krasovskii stability analysis, providing stronger theoretical guarantees.

In contrast to the optimized PID strategy in [43], where the controller gains are determined offline using patient-specific PK/PD models, the proposed MRAC updates its parameters automatically online and does not require model parameters for control implementation. In [43], the nonlinear BIS dynamics are handled through an explicit PK/PD–Hill model structure, and robustness is achieved via offline optimization over a population of virtual patients. However, physiological time delays are not explicitly modeled or addressed in the controller design or stability analysis. In contrast, the proposed method explicitly accounts for time-varying delays and achieves patient-independent regulation without the need for offline retuning.

Compared to the model predictive control strategies in [28] and [46], which rely on offline tuning and a fixed PK/PD predictor, the proposed MRAC automatically updates its control parameters online and does not require patient-specific model parameters for implementation. Moreover, in our MRAC approach, physiological time-varying delays are explicitly addressed in the control design and stability analysis. Additionally, unlike the nonlinear MPC approach in [28] and [46], the proposed method employs a simplified

inverse Hill reconstruction based on a proportional approximation of the combined drug effects, while preserving effective BIS tracking.

5. Conclusion

This work presents a novel Model Reference Adaptive Control (MRAC) approach for automated regulation of anesthesia depth through the coordinated dosing of propofol and remifentanil. The controller explicitly incorporates patient variability and time-varying delays into the pharmacokinetic/pharmacodynamic (PK/PD) modeling, enabling reliable, real-time closed-loop control without the need for patient-specific parameter identification. By integrating pharmacological patient models with an adaptive controller and an inverse nonlinear function, the proposed method accurately tracked the desired BIS level under inter-patient variability and time-varying delays. Its independence from patient-specific parameters, low computational complexity, and ability to handle physiological delays make it a scalable solution for closed-loop anesthesia systems. Future work will involve clinical validation and integration with broader anesthetic management strategies.

6. Funding statement

This work was supported by Isfahan University of Medical Sciences, Isfahan, Iran.

7. Ethics statement

This study is a simulation-based investigation and did not involve the recruitment of human participants, collection of patient data, clinical interventions, or animal experiments. The propofol parameters were obtained from a previously published virtual patient population [41], and the remifentanil pharmacokinetic/pharmacodynamic parameters were generated based on values reported in the literature [42]. No new patient data were collected or generated in the present study. Therefore, ethics committee approval and informed consent were not required. All methods were carried out in accordance with relevant guidelines and regulations.

8. Data availability statement

All data generated or analysed during this study are included in this published article.

9. Declaration of generative AI and AI-assisted technologies in the manuscript preparation process

In the preparation of this manuscript, ChatGPT (OpenAI) was utilized to enhance linguistic clarity and aid in English editing. The authors subsequently reviewed and revised the content, assuming full responsibility for the final published material.

10. CRediT authorship contribution statement

Raha Rahimi: Conceptualization, Methodology, Software, Validation, Formal analysis, Investigation, Resources, Data curation, Writing – original draft, Writing – review & editing, Visualization.

Marzieh Kamali: Conceptualization, Methodology, Validation, Writing – review & editing, Supervision, Project administration.

Farzaneh Shayegh: Conceptualization, Methodology, Validation, Writing – review & editing, Supervision, Project administration.

Zahra Baharlouei: Writing – review & editing, Funding acquisition.

11. Declaration of competing interests

The authors declare that they have no known competing financial interests or personal relationships that could have appeared to influence the work reported in this paper.

References

1. Martinez-Vazquez, P. & Jensen, E. W. Different perspectives for monitoring nociception during general anesthesia. *Korean Journal of Anesthesiology* vol. 75 112–123 at https://doi.org/10.4097/kja.22002 (2022).
2. Oh, S. S. & Narver, H. L. Mouse and Rat Anesthesia and Analgesia. *Curr. Protoc.* **4**, (2024).
3. Laferrière-Langlois *et al.* Depth of Anesthesia and Nociception Monitoring: Current State and Vision For 2050. *Anesth. Analg.* **2**, 295–307 (2024).
4. Park, S., Choi, S. L., Nahm, F. S., Ryu, J. H. & Do, S. H. Dexmedetomidine-remifentanil vs propofol-remifentanil for monitored anesthesia care during hysteroscopy Randomized, single-blind, controlled trial. *Med. (United States)* **99**, E22712 (2020).
5. Sabourdin, N. *et al.* Analgesia Nociception Index-Guided Remifentanil versus Standard Care during Propofol Anesthesia: A Randomized Controlled Trial. *J. Clin. Med.* (2022).
6. Grape, S., Kirkham, K. R., Frauenknecht, J. & Albrecht, E. Intra-operative analgesia with remifentanil vs. dexmedetomidine: a systematic review and meta-analysis with trial sequential analysis. *Anaesthesia* vol. 74 793–800 at https://doi.org/10.1111/anae.14657 (2019).
7. Jarrett, R. T., Blair, J. L. & Shotwell, M. S. Optimal BIS reference functions for closed-loop induction of anesthesia with propofol. *Comput. Biol. Med.* **144**, (2022).
8. Fuchs-Buder, T. *et al.* Peri-operative management of neuromuscular blockade: A guideline from the European Society of Anaesthesiology and Intensive Care. *Eur. J. Anaesthesiol.* **40**, 82–94 (2023).
9. Breshears, J. D. *et al.* Stable and dynamic cortical electrophysiology of induction and emergence with propofol anesthesia. *Proc. Natl. Acad. Sci. U. S. A.* **107**, 21170–21175 (2010).
10. Padula, F. *et al.* Optimized PID control of depth of hypnosis in anesthesia. *Comput. Methods Programs Biomed.* **144**, 21–35 (2017).
11. Schiavo, M., Padula, F., Latronico, N., Paltenghi, M. & Visioli, A. Experimental results of an event-based PID control system for propofol and remifentanil coadministration. *Control Eng. Pract.* **131**, (2023).
12. Kertai, M. D., Whitlock, E. L. & Avidan, M. S. Brain monitoring with electroencephalography and the electroencephalogram- derived bispectral index during cardiac surgery. *Anesthesia and Analgesia* vol. 114 533–543 at https://doi.org/10.1213/ANE.0b013e31823ee030 (2012).
13. Zaouter, C., Joosten, A., Rinehart, J., Struys, M. M. R. F. & Hemmerling, T. M. Autonomous systems in anesthesia: Where do we stand in 2020? A narrative review. *Anesth. Analg.* 1120–1132 (2020) doi:10.1213/ANE.0000000000004646.
14. Pawłowski, A., Schiavo, M., Latronico, N., Paltenghi, M. & Visioli, A. Event-based MPC for propofol administration in anesthesia. *Comput. Methods Programs Biomed.* **229**, (2023).
15. Warner, M. A. *et al.* Anesthesia Patient Safety: Next Steps to Improve Worldwide Perioperative

Safety by 2030. *Anesth. Analg.* **135**, 6–19 (2022).

16. Paolino, N., Schiavo, M. & Visioli, A. Biomedical Signal Processing and Control Kalman filter soft sensor to handle signal quality loss in closed-loop controlled anesthesia. *Biomed. Signal Process. Control* **104**, 107506 (2025).
17. Cardona García, M. C., Vallejo Santacruz, D. A., Valencia Vargas, D. F. & Valencia Murillo, J. F. 2018 IEEE ANDESCON : 22-24 August 2018, Santiago de Cali, Colombia. in 111 (Institute of Electrical and Electronics Engineers, 2018).
18. Dong, D. *et al.* Morbid obesity alters both pharmacokinetics and pharmacodynamics of propofol: Dosing recommendation for anesthesia induction. *Drug Metab. Dispos.* **44**, 1579–1583 (2016).
19. Gambús, P. L. & Trocõniz, I. F. Pharmacokinetic-pharmacodynamic modelling in anaesthesia. *Br. J. Clin. Pharmacol.* **79**, 72–84 (2015).
20. Chellaboina, V., Haddad, W. M., Ramakrishnan, J. & Hui, Q. Direct Adaptive Control of Nonnegative and Compartmental Dynamical Systems with Time Delay. *Springer-Verlag Berlin Heidelb.* 291–316 (2007).
21. Zou, H., Banerjee, P., Leung, S. S. Y. & Yan, X. Application of Pharmacokinetic-Pharmacodynamic Modeling in Drug Delivery: Development and Challenges. *Frontiers in Pharmacology* vol. 11 at https://doi.org/10.3389/fphar.2020.00997 (2020).
22. He, Y., Peng, S., Chen, M., Yang, Z. & Chen, Y. A Transformer-Based Prediction Method for Depth of Anesthesia During Target-Controlled Infusion of Propofol and Remifentanil. *IEEE Trans. Neural Syst. Rehabil. Eng.* **31**, 3363–3374 (2023).
23. Russell, D. *et al. Manual Compared with Target-Controlled Infusion of Propofol*. *British Journal of Anaesthesia* vol. 75 (1995).
24. Copot, D., Ghita, M., Birs, I. & Cajo, R. Closed-loop control of multi-drug infusion for anesthesia and hemodynamic management. in *2022 IEEE Conference on Control Technology and Applications, CCTA 2022* 1111–1116 (Institute of Electrical and Electronics Engineers Inc., 2022). doi:10.1109/CCTA49430.2022.9966032.
25. Ghita, M., Neckebroek, M., Muresan, C. & Copot, D. Closed-loop control of anesthesia: Survey on actual trends, challenges and perspectives. *IEEE Access* **8**, 206264–206279 (2020).
26. Schiavo, M. *et al.* Biomedical Signal Processing and Control Optimized feedforward control of propofol for induction of hypnosis in general anesthesia. *Biomed. Signal Process. Control* **66**, 102476 (2021).
27. Savoca, A. & Manca, D. Biomedical Signal Processing and Control A physiologically-based approach to model-predictive control of anesthesia and analgesia. *Biomed. Signal Process. Control* **53**, 101553 (2019).
28. Pawłowski, A., Schiavo, M., Latronico, N., Paltenghi, M. & Visioli, A. Model predictive control using MISO approach for drug co-administration in anesthesia. *J. Process Control* **117**, 98–111 (2022).
29. L´opez-Ram´ırez, A., Gallardo-Hern´andez, A. G. & Escobar, J. Design and Simulation of a Sliding Mode Control for Anesthesia. *IEEE Lat. Am. Trans.* **23**, (2025).
30. Navarro-Guerrero, G. & Tang, Y. Fractional order model reference adaptive control for anesthesia. *Int. J. Adapt. Control Signal Process.* **31**, 1350–1360 (2017).
31. Soltesz, K., Van Heusden, K. & Dumont, G. A. Models for control of intravenous anesthesia. in *Automated Drug Delivery in Anesthesia* 119–166 (Elsevier, 2020). doi:10.1016/B978-0-12-815975-0.00010-2.

32. Soltesz, K., Hahn, J. O., Dumont, G. A. & Ansermino, J. M. Individualized PID control of depth of anesthesia based on patient model identification during the induction phase of anesthesia. in *Proceedings of the IEEE Conference on Decision and Control* 855–860 (Institute of Electrical and Electronics Engineers Inc., 2011). doi:10.1109/CDC.2011.6160189.

33. Bouillon, T. *et al. Non-Steady State Analysis of the Pharmacokinetic Interaction between Propofol and Remifentanil*. *Anesthesiology* vol. 97 http://anesthesia.stanford.edu/pkpd/. (2002).

34. Bouillon, T. W. *et al. Pharmacodynamic Interaction between Propofol and Remifentanil Regarding Hypnosis, Tolerance of Laryngoscopy, Bispectral Index, and Electroencephalographic Approximate Entropy*. *Anesthesiology* vol. 100 (2004).

35. Koitabashi, T., Johansen, J. W. & Sebel, P. S. *Remifentanil Dose/Electroencephalogram Bispectral Response During Combined Propofol/Regional Anesthesia*. *Anesth Analg* vol. 94 (2002).

36. Schnider, T. et al. The influence of age on propofol pharmacodynamics. *J. Am. Soc. Anesthesiol.* **90**, 1502–1516 (1999).

37. Schnider, T. et al. The influence of method of administration and covariates on the pharmacokinetics of propofol in adult volunteers. *J. Am. Soc. Anesthesiol.* **88**, 1170–1182 (1998).

38. Ioannou, P. et al. *Robust Adaptive Control*. (Courier Corporation, 2012).

39. Mirkin, B. & Gutman, O. *Robust Adaptive Output-Feedback Tracking: The Case of Linear State-Delayed Plants*.

40. Kamali, M., Askari, J. & Sheikholeslam, F. An output-feedback adaptive actuator failure compensation controller for systems with unknown state delays. *Nonlinear Dyn.* **67**, 2397–2410 (2012).

41. Nascu, I., Nascu, I., Ionescu, C. M. & De Keyser, R. Adaptive EPSAC Predictive Control of the Hypnotic Component in Anesthesia. in *Proceedings of 2012 IEEE International Conference on Automation, Quality and Testing, Robotics, Cluj-Napoca, Romania* (2012).

42. Kern, S. E. *Opioid-Hypnotic Synergy A Response Surface Analysis of Propofol-Remifentanil Pharmacodynamic Interaction in Volunteers*. *Anesthesiology* vol. 100 http://anesthesia.stanford.edu/ (2004).

43. Merigo, L., Padula, F., Latronico, N., Paltenghi, M. & Visioli, A. Optimized PID control of propofol and remifentanil coadministration for general anesthesia. *Commun. Nonlinear Sci. Numer. Simul.* **72**, 194–212 (2019).

44. Landau, I. D., Lozano, R., M'Saad, M. & Karimi, A. *Adaptive Control*. (Springer London, London, 2011). doi:10.1007/978-0-85729-664-1.

45. Struys, M. M. *26. Intravenous Drug Delivery Systems Intravenous Drug Delivery Systems Key Points* ▪.

46. Pawłowski, A., Schiavo, M., Latronico, N., Paltenghi, M. & Visioli, A. Drug co-administration in anesthesia using event-based MPC. 4020–4042 (2025) doi:10.1002/rnc.7080.